DRAG REDUCTION BEHIND A BLUFF BODY

Parth Batra[1], Gaurav Kumar[1], Kishlay Srivastava[1], and M.B. Shyam Kumar[2]

[1]Student, Bachelor of Technology, School of Mechanical and Building Sciences, VIT University, Chennai, India

[2]Associate Professor, School of Mechanical and Building Sciences, VIT University, Chennai, India

ABSTRACT: The present paper focus on reduction of drag force behind a bluff body by using a passive method. Numerical simulations have been carried out for ten different isolated cylindrical geometries at a Reynolds number of 100. Influences of corner radii on the drag force behind a two dimensional bluff body have been investigated using ANSYS FLUENT. It was found that the critical radius at which the drag force turned to be minimum compared to the circular cylinder was R=D/3. The results in terms of the bulk parameters like time history of drag and lift coefficients, Strouhal number, recirculation length and contours of pressure, vorticity and streamlines have been discussed.

KEYWORDS: Bluff body, Reynolds number, Rounded corner, Passive method, Drag, Lift, CFD, Vortex shedding.

1 INTRODUCTION

The flow around a slender cylindrical bluff body has been the subject of intense research over many years and also one of the interesting fluid structure interaction problems in engineering. Due to its significance in structural design and flow induced vibration, advancement in computer technology and good experimental techniques, in recent years these studies have got a great deal of attention. There are many structures that have rectangular or near rectangular cross sections that include architectural features on buildings, beams & fences etc.

In today's world most of the vehicles, ships and airplanes have highly engineered geometry to minimize the drag force due to its great impact on fuel consumption. As mentioned by Hsu and Davis [1], it is estimated that with a drag reduction of about 40%, 10,000 USD/year/vehicle can be saved. The body facing high amount of drag force consumes more fuel and faces difficulty in motion. In order to reduce the drag force, two techniques namely the Active and Passive methods are available as shown in Figure 1.
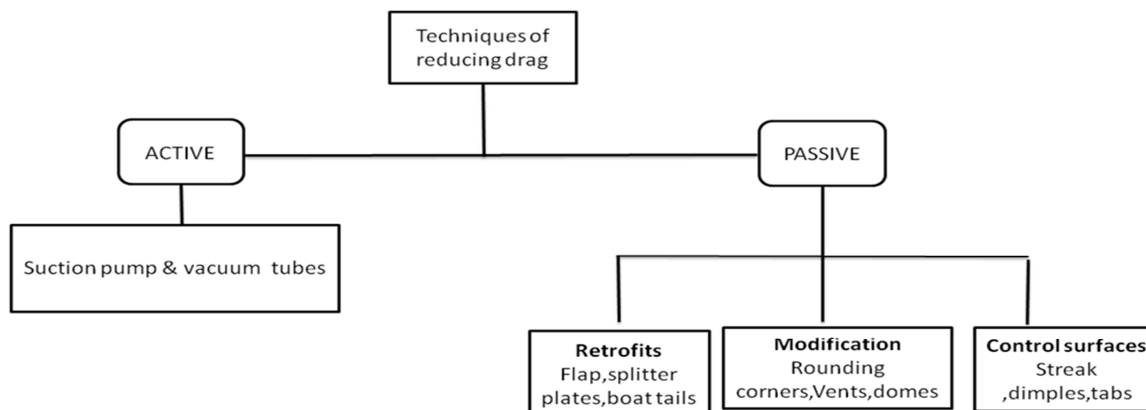
Figure 1: Active and Passive Method

Many researchers have studied the flow past circular cylinder at low Reynolds number [2-5].They studied parameters like Strouhal number, mean drag coefficient, length of bubble recirculation and RMS value of lift coefficient for several values of Reynolds number. They aimed at understanding the two dimensional and three dimensional vertical instabilities in the circular cylinder wake. Studies have been conducted on square cylinder with the secondary instability region of mode A and mode B [6]. From the understanding through literature it is found that flow separation has significant effect on the drag force. While the flow separation is fixed at the upstream sharp corners for a square cylinder, the flow separation takes place in the downstream part of a circular cylinder. Thus a wider wake is formed behind a square cylinder creating a larger drag in comparison with that of a circular cylinder. In order to reduce the drag behind a square cylinder, few researchers have used some passive methods [7-11]. To the best of our knowledge, reducing drag behind a square cylinder by rounding the sharp corners has not been reported. Thus the main aim of this paper would be to find the critical radius at which the drag generated is minimum.

2   METHODOLOGY

The numerical simulations for flow past different bluff body configurations such as circular cylinder, square cylinder and square cylinder with eight corner radii have been studied at Reynolds number of 100 using ANSYS FLUENT software.

2.1   GOVERNING EQUATIONS AND BOUNDARY CONDITIONS

A uniform, viscous and incompressible fluid flow with constant fluid properties is considered for a two dimensional geometry. The equations for continuity and momentum may be articulated in the dimensionless form as follows:

Continuity:

$$\frac{\partial u}{\partial x} + \frac{\partial v}{\partial y} = 0$$

X-momentum:

$$\frac{\partial u}{\partial t} + u\frac{\partial u}{\partial x} + v\frac{\partial u}{\partial y} = -\frac{\partial p}{\partial x} + \frac{1}{Re}\left(\frac{\partial^2 u}{\partial x^2} + \frac{\partial^2 u}{\partial y^2}\right)$$

Y-momentum:

$$\frac{\partial v}{\partial t} + u\frac{\partial v}{\partial x} + v\frac{\partial v}{\partial y} = -\frac{\partial p}{\partial y} + \frac{1}{Re}\left(\frac{\partial^2 v}{\partial x^2} + \frac{\partial^2 v}{\partial y^2}\right)$$

In the above equations u, v and p represents the instantaneous velocity components and pressure, respectively. A computational domain of size 27D x 18D along with boundary conditions (Table 1) is shown in Figure 2 and the flow is from left to right. The origin is at the centre of square cylinder. Here X and Y denote the streamwise and cross streamwise directions respectively. The domain length for upstream flow is 8.5D and for downstream it is 17.5D. At inlet, a uniform velocity is taken as (U∞ =1.4607 m/s) for Re=100 and convective boundary condition is used at the outlet. The top and bottom boundary are given slip condition whereas no slip is given for square cylinder to attain boundary layer effect at the periphery of cylinder.

The grid points near the square cylinders are uniformly distributed while they are stretched gradually in the other regions of minor interest (Figure 3). For this study, the distance of first grid point was taken as 0.04D, where D=0.1m. To carry out the grid refinement study, three different grid sizes were made and the results are shown in Table 2. In stated grid sizes, the one which gave less percentage error with less mesh counts was taken for the all the simulations.

3 FORMULAE USED

$Re = \dfrac{\rho U_\infty D}{\mu}$, where Re = Reynolds number, U_∞ = inlet velocity, D = cylinder diameter

and μ = absolute vis cos ity

$St = \dfrac{f\,D}{U_\infty}$, where f = vortex shedding frequency
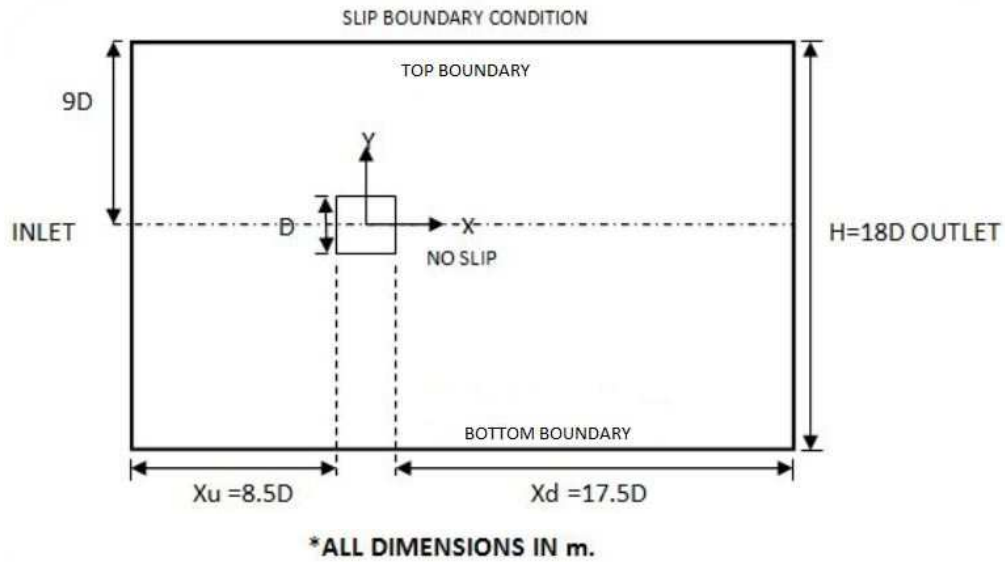
Figure 2: Computational domain along with the boundary conditions
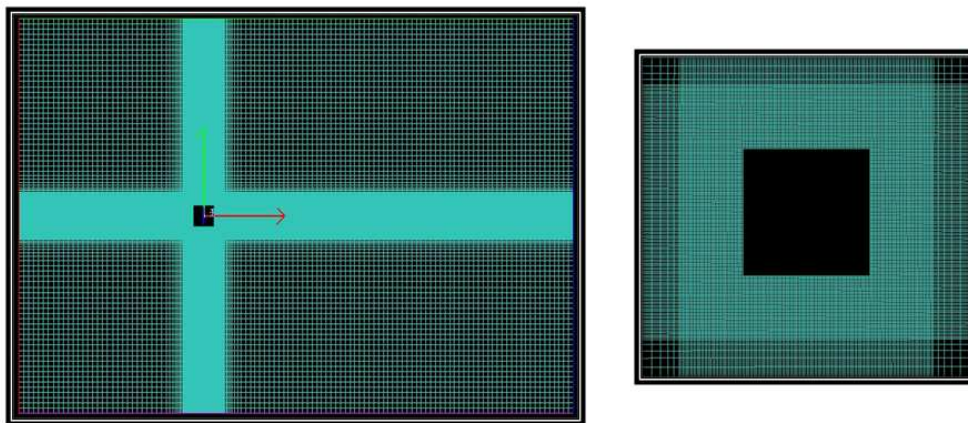
Figure 3: A grid of size 300 x 260 used for computation

Table 1: Boundary Conditions

Medium	Air
Density	1.225 kg/m^3
Reynolds number	100
Inlet conditions	Velocity inlet
Outlet	Convective/ Outflow
Velocity at inlet	1.4607 m/s
Solution method	Unsteady
Time step	0.05
Angle of incidence	0^0
Mesh type	Quadrilateral

Table 2: Grid Independency Study

Sl. No.	GRID SIZE	Sohankar et al., [12] $\overline{C_D}$	Present Data $\overline{C_D}$	% ERROR
1.	270 x 240	1.478	1.433	3.04
2.	300 x 260	1.478	1.467	0.74
3.	330 x 280	1.478	1.470	0.54
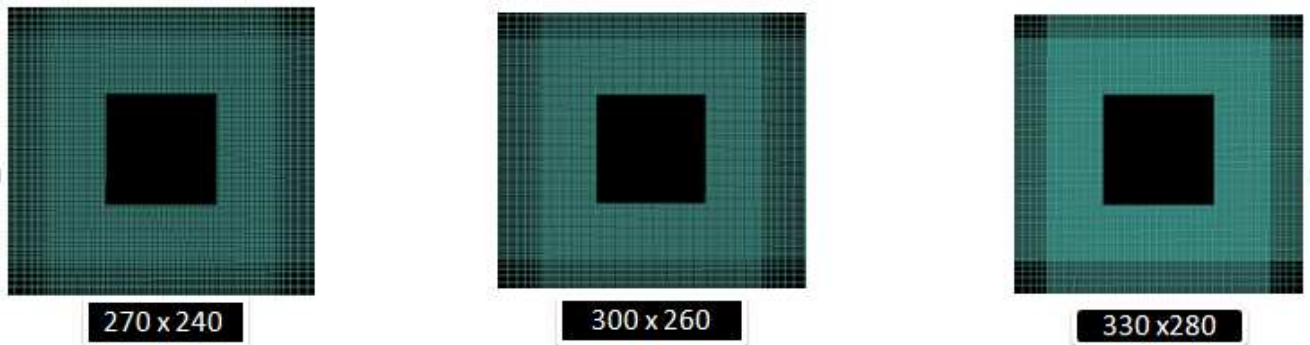
Figure 4: Magnified view of grids used around the cylinder
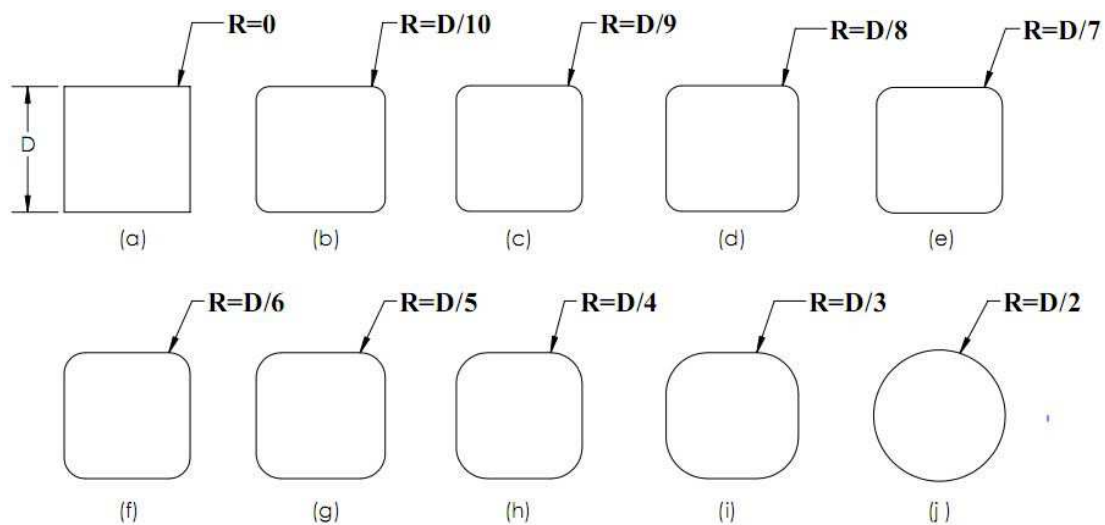
Figure 5: Different Configurations

4   VALIDATION STUDIES

The numerical simulation has been validated for two cases (i) flow past square cylinder at Re=100 and (ii) flow over circular cylinder at Re=100. Table 3 presents the comparison of present value and literature. It is found that the results are in good agreement with those reported in the literature.

Table 3: Validation

Author	$\overline{C_D}$	C_L^{RMS}	St
Circular cylinder at Re=100			
Present data	1.337	0.159	0.165
Rajani et al., [3]	1.335	0.179	0.157
Silva et al., [2]	1.390	-	-
Saha et al., [6]	-	0.122	-
Square cylinder at Re=100			
Present data	1.467	0.127	0.119
Gera et al., [12]	1.461	0.157	0.129
Sohankar et al., [5]	1.478	0.130	0.146
Robichaux et al.[13]	1.53	-	0.154

5   RESULTS AND DISCUSSION

Numerical simulations were done in ANSYS FLUENT software for ten different configurations as shown in Figure 5. The simulations involved the flow of air at Reynolds number of 100. The simulations were carried out for a total flow time of 250s with a time step size of 0.05s.

The bulk parameters namely the mean drag coefficient, RMS lift coefficient and Strouhal number are presented in Table 4. The time histories of C_D and C_L for the flow past different cylinders are shown in Figure 7 and Figure 8 respectively. They show periodic oscillations of low frequency. Results of the present work show that the square cylinder with corner radius R=D/3 has the coefficient of drag value less than the circular cylinder as shown in Figure 6. From Figure 8 we can infer that mean lift coefficient is zero which implies no lift forces are generated for any of the configurations.

Table 4: Bulk Parameters

Configuration Number	Fillet Radius, R	$\overline{C_D}$	C_L^{RMS}	St
0	0	1.467	0.127	0.119
1	D/10	1.426	0.177	0.103
2	D/9	1.416	0.177	0.107
3	D/8	1.408	0.150	0.123
4	D/7	1.398	0.175	0.111
5	D/6	1.396	0.161	0.136
6	D/5	1.380	0.172	0.116
7	D/4	1.368	0.148	0.164
8	**D/3**	**1.328**	**0.100**	**0.191**
9	D/2	1.337	0.159	0.165
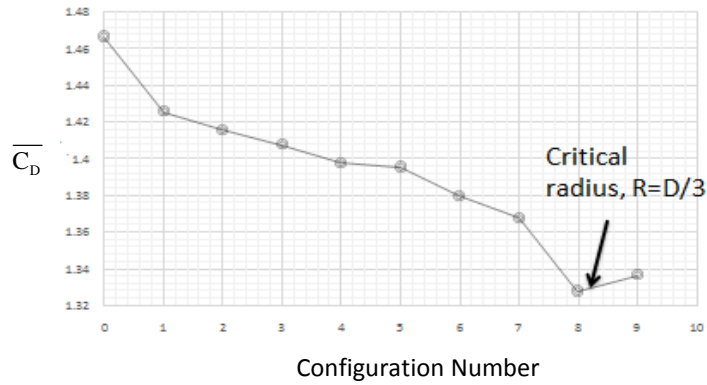
Figure 6: Influence of corner radii on mean drag coefficient
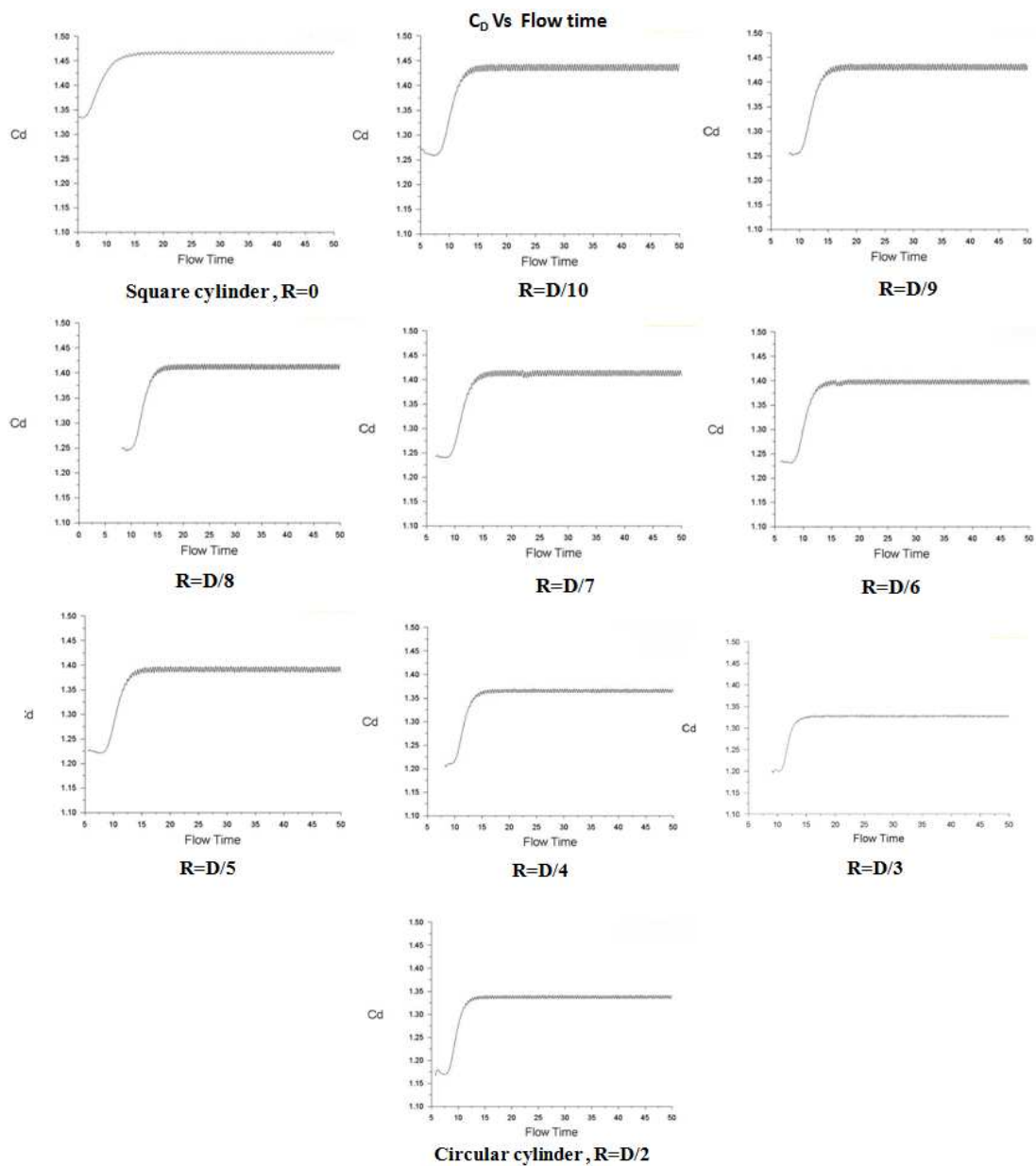
Figure 7: Drag Coefficient as function of flow time for different geometries
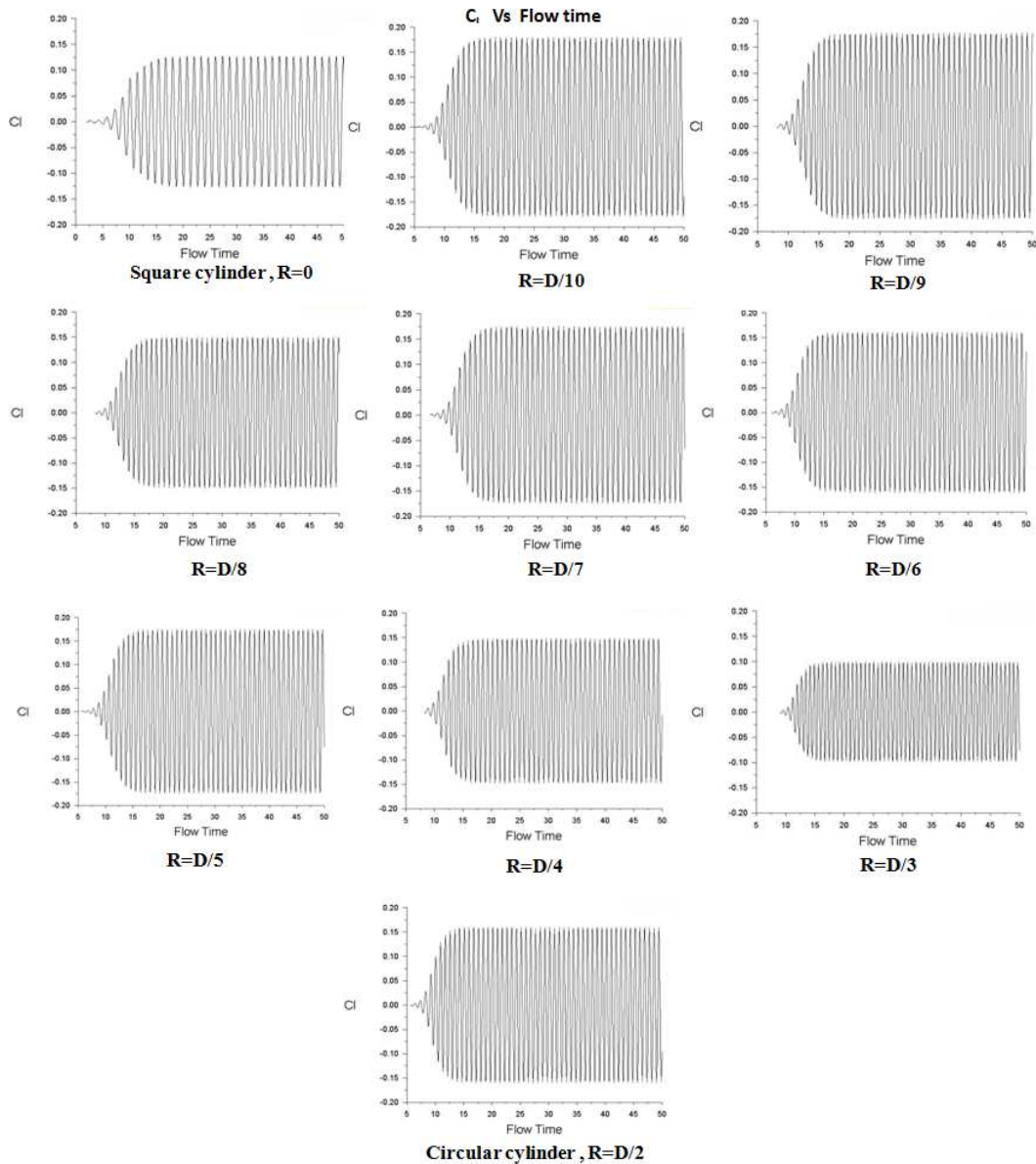
Figure 8: Lift Coefficient as function of flow time for different geometries

The non-dimensional vortex shedding frequency is defined by Strouhal number, $St = (fD)/U_\infty$ where f is vortex shedding frequency, D is diameter of cylinder and U_∞ is free stream inlet velocity. The Strouhal number for square cylinder with rounded corner R=D/3 is found to be more than the circular cylinder as shown in Table 4.

The plots of coefficient of pressure on the cylinder surface for various configurations are shown in Figure 9. From these plots, it can be observed that the stagnation point at position 1 has the highest value with respect to all other points. The plot is symmetric about front stagnation point. For all the configurations, the mean static pressure contour Figure 10, shows a maximum value at the stagnation pressure and a minimum value in the wake which contributes to the drag force. Vorticity is defined as the measure of rotation in atmosphere or "spin" in air. Figure 11 shows the instantaneous vorticity plots for the different configurations studied. The vortex shedding phenomenon along with Von Karman vortex street flow pattern are clearly observed. Other phenomena namely the vortex pairing, splitting and tearing are also observed.
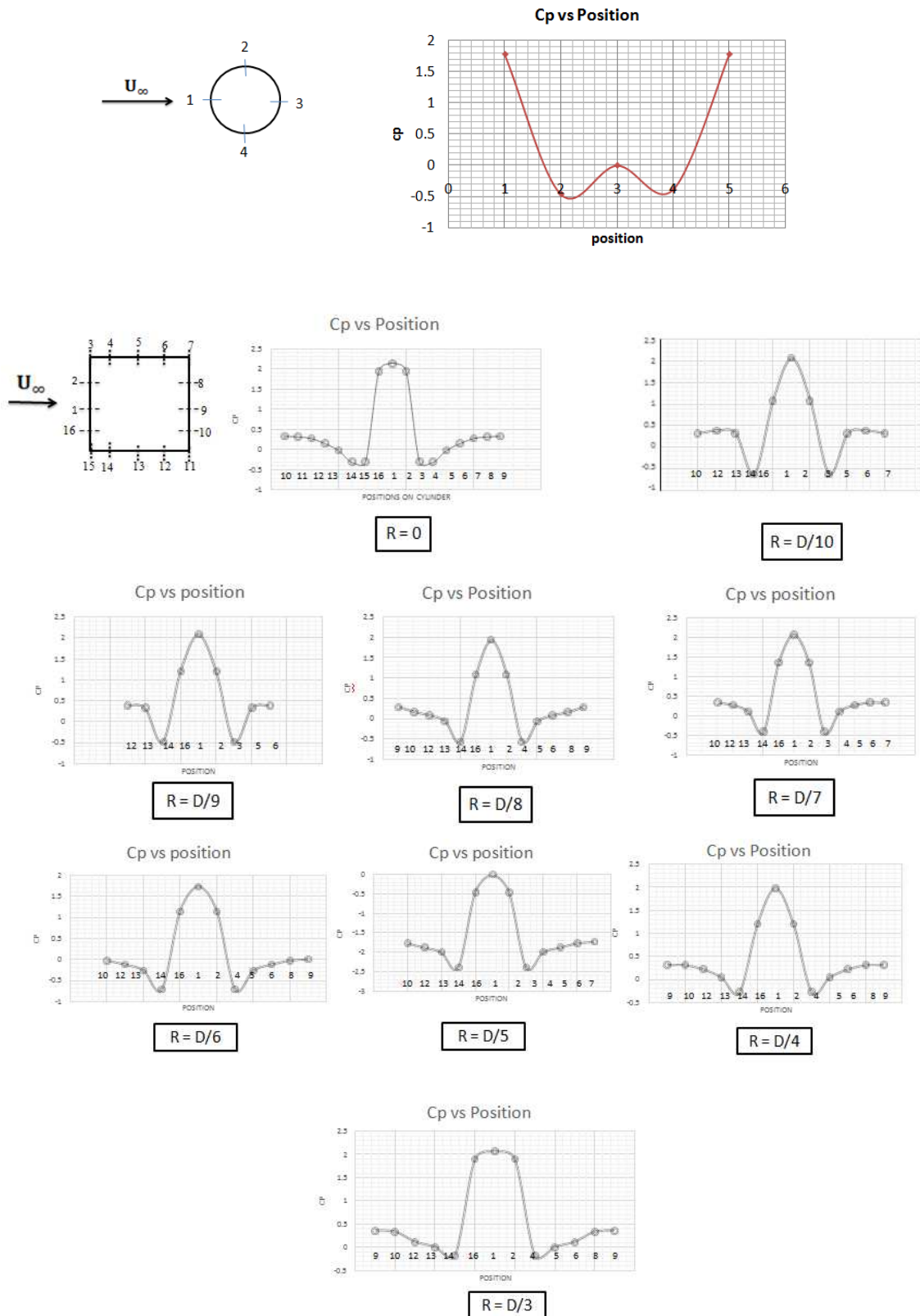
Figure 9: Pressure coefficients on the cylinder surface
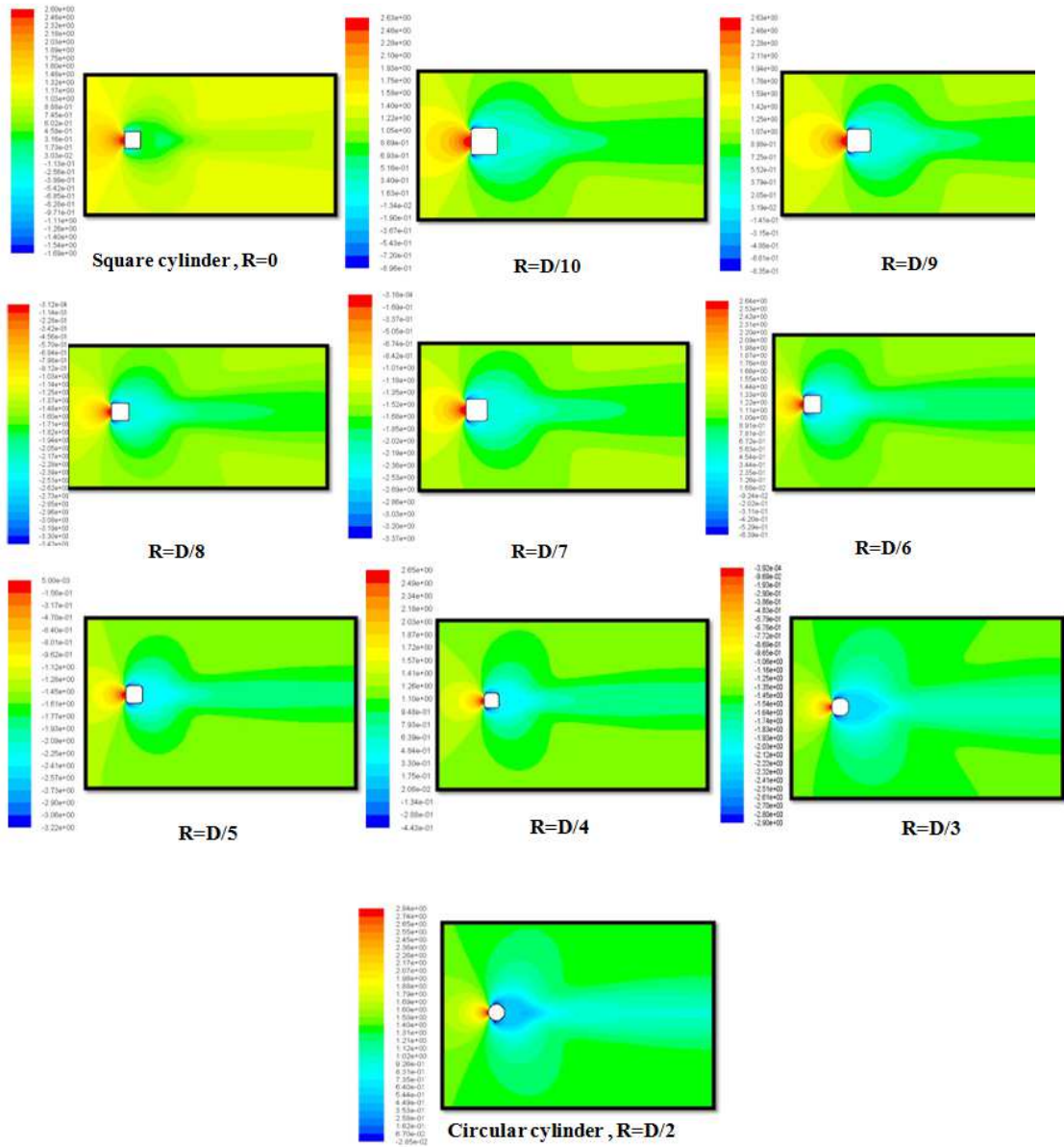
Figure 10: Contour of static pressure
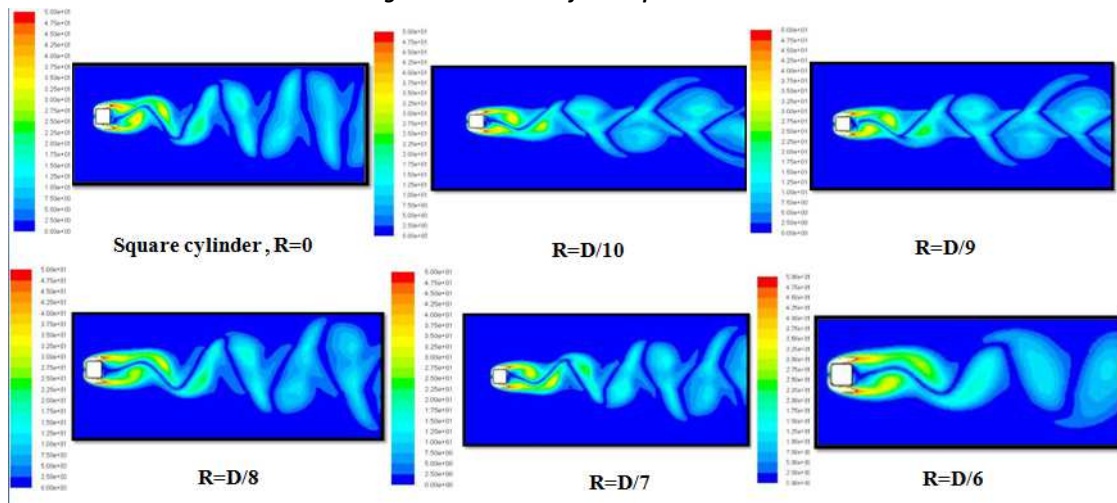
Figure 11: Contour of instantaneous vorticity
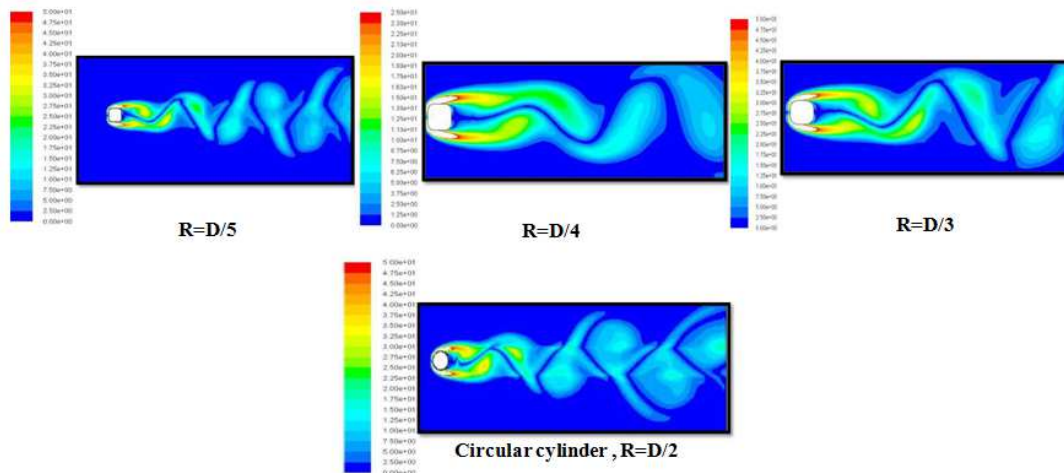
Figure 11: Contour of instantaneous vorticity (Contd.)

Figure 12 shows the instantaneous streamline contours for the different configurations studied. The wake formation behind the cylinders is clearly visible using which the length of bubble recirculation is calculated and tabulated in Table 5. From this table, it was found that the length of bubble recirculation for square cylinder with rounded corner R=D/3 is least whereas for a perfect square cylinder it is maximum.
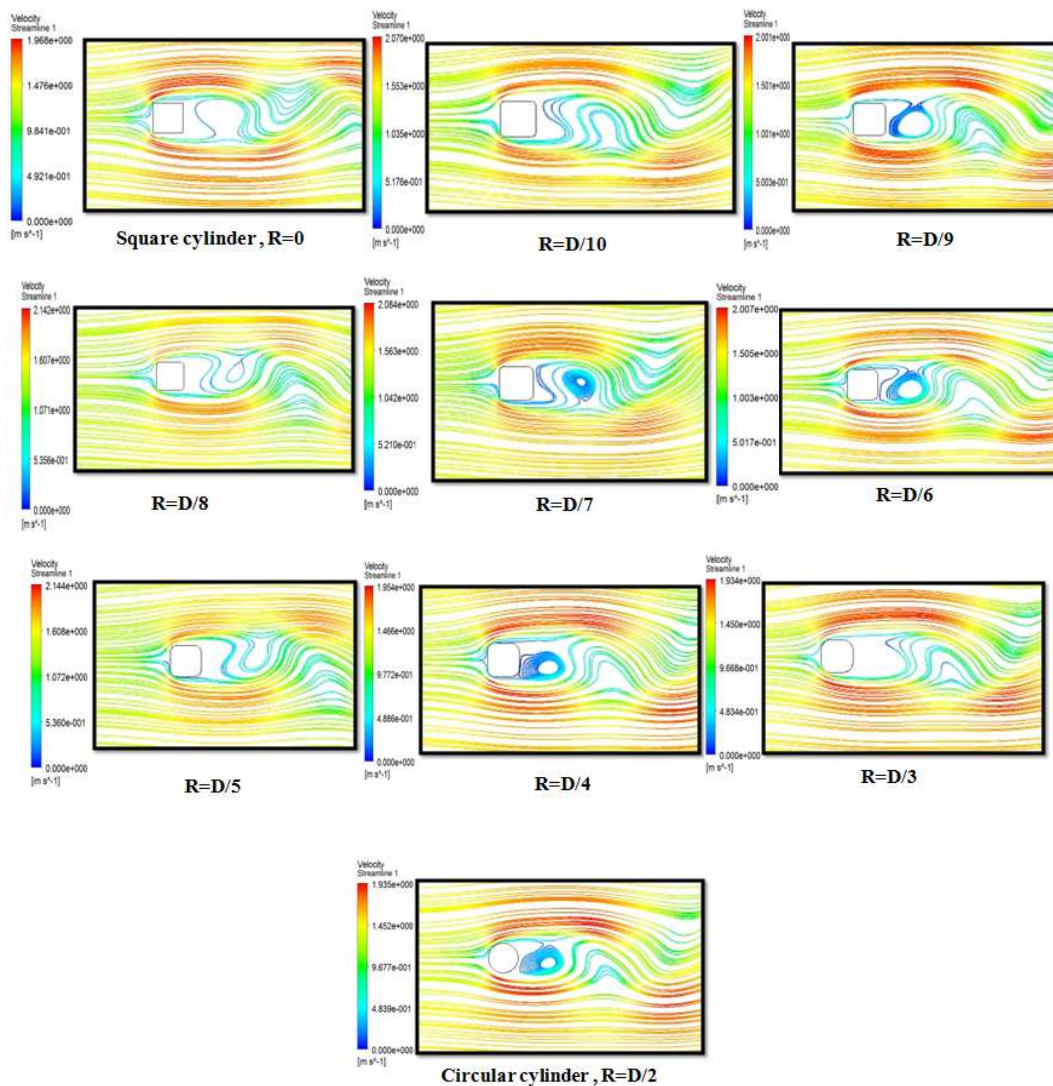
Figure 12: Instantaneous streamline contour at Re=100.
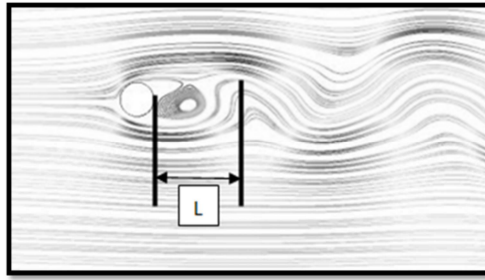
Figure 13: Length of the bubble recirculation

Table 5: Fillet radius with length of bubble recirculation

SI .No.	Fillet radius	Length of bubble recirculation (L in m)
1.	R=0	0.286
2.	R=D/10	0.278
3.	R=D/9	0.281
4.	R=D/8	0.256
5.	R=D/7	0.246
6.	R=D/6	0.244
7.	R=D/5	0.256
8.	R=D/4	0.213
9.	R=D/3	0.206
10.	R=D/2	0.212

6   CONCLUSIONS

A detailed numerical investigation was carried out to study the effect of square cylinder corner radii on the drag coefficient at Reynolds number 100. The simulations were performed on ten different configurations ranging from corner radius R=0(Square cylinder) to R=D/2(circular cylinder). The validation studies carried out were found to be in very good agreement with those reported in the literature. It is understood from the above numerical simulations that by making the corners of the square cylinder rounded there is a drastic reduction in the drag forces generated behind the cylinders. In the carried out simulations, the square cylinder with rounded corner R=D/3 was found to be the critical radius at which drag coefficient was even lesser than the corresponding value for circular cylinder.

REFERENCES

[1]   F. H. Hsu and R. L. Davis, "Drag reduction of tractor-trailers using optimized add-on devices", *Journal of Fluids Engineering*, vol. 132, no. 8, 084504. doi:10.1115/1.4001587.

[2]   A. L. F. Lima E Silva, A. Silveira-Neto and J. J. R. Damasceno, "Numerical simulation of two-dimensional flow over a circular cylinder using the immersed boundary method", *Journal of Computational Physics*, vol. 189, pp. 351–370, 2003.

[3]   B. N. Rajani, A. Kandasamy, and Sekhar Majumdar, "Numerical simulation of laminar flow past a circular cylinder", *Applied Mathematical Modeling*, vol. 33, pp.1228–1247, 2009.

[4]   C. Y. Wen, C. L. Yeh, M. J. Wang and C. Y. Lin, "On the drag of two-dimensional flow about a circular cylinder", *Physics of Fluids*, vol. 16, pp. 3828-3831, 2004.

[5]   A. Sohankar, C. Norberg and L. Davidson, "Low Reynolds Number Flow around a Square Cylinder at Incidence: Study of Blockage, Onset of Vortex Shedding and Outlet Boundary Condition", *International Journal for Numerical Methods in Fluids*, vol. 26, pp. 39-56, 1998.

[6]   A. K. Saha, G. Biswas and K. Muralidhar, "Three-dimensional study of flow past a square cylinder at low Reynolds numbers", *International Journal of Heat and Fluid Flow*, vol. 24, pp. 54–66, 2003.

[7]   M. B. Shyam Kumar and S. Vengadesan, "Influence of Rounded Corners on Flow Interference Due to Square Cylinders Using Immersed Boundary Method", *Journal of Fluids Engineering*, vol. 134, pp. 1-23, 2012.

[8] Alaman Altaf, Ashraf A Omar and Waqar Asrar, "Review of passive drag reduction techniques for bluff road vehicles", *IIUM Engineering Journal*, vol. 15, pp. 1-69, 2014.

[9] Jong-Yeon Hwang and Kyung-Soo Yang, "Drag reduction on a circular cylinder using dual detached splitter plates", *Journal of Wind Engineering and Industrial Aerodynamics*, vol.95, pp. 551–564, 2007.

[10] P. W. Bearman, J. M. R. Graham, E. D. Obasaju and G. M. Drossopoulos, "The Influence of Corner Radius on the Forces Experienced by Cylindrical Bluff Bodies in Oscillatory Flow", *Appl. Ocean. Res*., vol. 6, pp. 83–89, 1984.

[11] C. Dalton and W. Zheng, "Numerical Solutions of a Viscous Uniform Approach Flow Past Square and Diamond Cylinders", *J. of Fluids and Structures*, vol. 18, pp. 455–465, 2003.

[12] B. Gera, Pavan K Sharma and R. K. Singh, "CFD analysis of 2D unsteady flow around a square cylinder", *International Journal of Applied Engineering Research*, vol. 1, pp. 602-609, 2010.

[13] J. Robichaux, S. Balachandar, and S. P. Vanka, "Three-dimensional Floquet instability of the wake of square cylinder", *Phys. of Fluids*, vol. 11, pp. 560-578, 1993.